JCB Article

Nudel functions in membrane traffic mainly through association with Lis1 and cytoplasmic dynein

Yun Liang, Wei Yu, Yan Li, Zhenye Yang, Xiumin Yan, Qiongping Huang, and Xueliang Zhu

Laboratory of Molecular Cell Biology, Institute of Biochemistry and Cell Biology, Shanghai Institutes for Biological Sciences, Chinese Academy of Sciences, Shanghai 200031, China

Nudel and Lis1 appear to regulate cytoplasmic dynein in neuronal migration and mitosis through direct interactions. However, whether or not they regulate other functions of dynein remains elusive. Herein, overexpression of a Nudel mutant defective in association with either Lis1 or dynein heavy chain is shown to cause dispersions of membranous organelles whose trafficking depends on dynein. In contrast, the wild-type Nudel and the double mutant that binds to neither protein are much less effective. Time-lapse microscopy for lysosomes reveals significant reduction in both frequencies and velocities of their minus end–directed motions in cells expressing the dynein-binding defective mutant, whereas neither the durations of movement nor the plus end–directed motility is considerably altered. Moreover, silencing Nudel expression by RNA interference results in Golgi apparatus fragmentation and cell death. Together, it is concluded that Nudel is critical for dynein motor activity in membrane transport and possibly other cellular activities through interactions with both Lis1 and dynein heavy chain.

Introduction

Membrane traffic in animal cells is a highly dynamic process important for intracellular transport to and from various membrane organelles and plasma membranes (Lodish et al., 2000). In the secretory pathway, membrane vesicles emerged from the ER, namely the ER-to-Golgi intermediate compartment (ERGIC), deliver nascent secretory or membrane proteins to the cis faces of the Golgi complex for posttranslational modifications such as glycosylation. Modified proteins are transported to trans-Golgi cisternae and packed in secretory vesicles for fusion with the plasma membrane. In the endocytic pathway, membrane proteins or extracellular materials are internalized from the plasma membrane into endosomes, which are driven centripetally to fuse with either lysosomes or trans-Golgi cisternae. Instead of passive diffusion, these organelles are actively transported and organized by molecular motors (Hirokawa, 1998; Karki and Holzbaur, 1999).

Cytoplasmic dynein, a microtubule (MT)-based and minus end–directed motor, is a large complex composed of two dynein heavy chains (DHCs) of ~550 kD, three to four dynein intermediate chains (DICs) of 74 kD, four light intermediate chains of ~55 kD, and light chains of 8–22 kD (Hirokawa, 1998; Karki and Holzbaur, 1999). It exerts multiple functions, from the movement of chromosomes, formation and maintenance of the mitotic spindle during mitosis (Karki and Holzbaur, 1999; Brunet and Vernos, 2001) to centripetal transit and juxta-centrosomal distributions of membranous organelles, including the Golgi apparatus, ERGIC, endosomes, and lysosomes (Hirokawa, 1998; Karki and Holzbaur, 1999). Subtle mutations in DHC can specifically cause motor neuron degeneration diseases correlated with defects in the axonal retrograde transport and abnormal migration (Hafezparast et al., 2003). It is believed that cytoplasmic dynein anchors to its target sites through interaction with dynactin, another multisubunit complex (Holleran et al., 1998). However, how its motor activity is regulated is not fully understood.

In *Aspergillus nidulans*, even distribution of fungal nuclei along hypha requires a group of nuclear distribution factors. Among them are dynein subunits (e.g., NudA and NudG), NudE, and NudF, the fungal orthologue of mammalian Lis1 (Xiang et al., 1994, 1995; Willins et al., 1997; Efimov and Morris, 2000). NudE and NudF appear to be regulators of dynein. Lis1 is a WD-40 repeat protein whose complete

Y. Liang and W. Yu contributed equally to this work.

The online version of this article includes supplemental material.

Address correspondence to Xueliang Zhu, Institute of Biochemistry and Cell Biology, 320 Yue Yang Rd., Shanghai 200031, China. Tel.: 86-21-54921406. Fax: 86-21-54921011. email: xlzhu@sibs.ac.cn

Key words: NudE; organelle; motility; time-lapse microscopy; RNA interference

Abbreviations used in this paper: DHC, dynein heavy chain; DIC, dynein intermediate chain; ERGIC, ER-to-Golgi intermediate compartment; hPL, human placental lactogen; MT, microtubule; RNAi, RNA interference; SiRNA, small interference RNA; Tet, tetracycline.

loss results in early embryonic lethality in mice (Hirotsune et al., 1998). Moreover, human heterozygotes of Lis1 mutations suffer from type I lissencephaly, a severe congenital disease with smooth brain surfaces and disorganized cortical layering of the central nervous system due to neuronal migration defects (Hirotsune et al., 1998; Wynshaw-Boris and Gambello, 2001; Gupta et al., 2002). NudE is also conserved in eukaryotes, with two isoforms in mammals, NudE and Nudel (for NudE-like). Both proteins partially localize to the centrosome and are likely to have similar functions (Feng et al., 2000; Niethammer et al., 2000; Sasaki et al., 2000; Yan et al., 2003). Lis1, NudE/Nudel, and dynein interact with each other directly (Feng et al., 2000; Niethammer et al., 2000; Sasaki et al., 2000; Tai et al., 2002). Nudel is also a substrate of Cdk5/p35, a brain-specific kinase critical for neuronal migration, which is suggestive of a linker between the Cdk5 and dynein pathways (Niethammer et al., 2000; Sasaki et al., 2000). 14-3-3ε, a member in the ubiquitous phosphoserine/threonine-binding protein 14-3-3 family, associates with Cdk5/p35-phosphorylated Nudel and protects the latter from dephosphorylation (Toyo-oka et al., 2003). Haploinsufficiencies of both Lis1 and 14-3-3ε are implicated in neuronal migration defects more severe than lack of Lis1 alone (Toyo-oka et al., 2003). These lines of evidence suggest that Lis1 and NudE/Nudel function in neuronal migration through an evolutionarily conserved dynein pathway (Wynshaw-Boris and Gambello, 2001; Gupta et al., 2002).

We recently showed that Nudel is functionally involved in dynein-mediated poleward transport of kinetochore proteins, a process contributing to inactivation of the spindle checkpoint (Howell et al., 2001) in mitosis (Yan et al., 2003; Yang et al., 2003). Nudel and NudE are phosphorylated in M phase by Cdc2 and probably Erk1/2 (Yan et al., 2003). Nevertheless, the significance of Nudel–dynein interaction has not been tested. Whether or not Nudel functions in membrane traffic also remains unknown.

Results

Disruption of the Lis1 and DHC-binding domains of Nudel

To explore whether Nudel was involved in membrane trafficking and whether such a role was related to dynein and Lis1, we constructed mutants to hopefully study their dominant-negative effects (Fig. 1 A). We have previously shown that Nudel^{N20}, a Lis1-binding defective Nudel mutant lacking amino acids 114–133, impairs dynein-mediated protein transport along the mitotic spindle (Yan et al., 2003; Yang et al., 2003). Residues 256–291, essential for binding to DHC in yeast two-hybrid assays (Sasaki et al., 2000), were deleted to create another mutant, Nudel^{C36}. A double deletion mutant, Nudel$^{N20/C36}$, was also created to evaluate the effects of the remaining domains.

Consistent with previous works (Niethammer et al., 2000; Sasaki et al., 2000; Yan et al., 2003), FLAG-Nudel immunoprecipitated endogenous Lis1, DHC, DIC, and dynamitin, a dynactin subunit (Fig. 1 B, lane 7). γ- and α-tubulin also existed in the complex (Fig. 1 B, lane 7), despite some nonspecific binding of γ-tubulin (Fig. 1 B, lanes 6–10) and an additional band of ~55 kD (Fig. 1 B, lane 7),

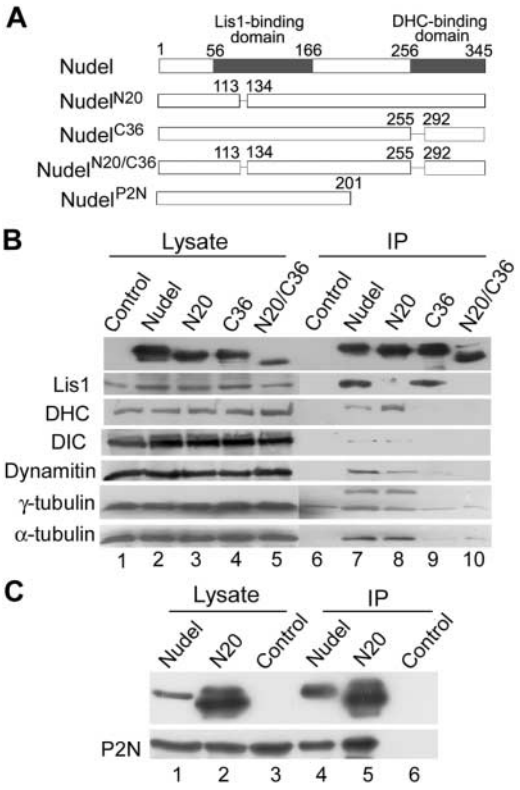

Figure 1. **Biochemical properties of Nudel mutants.** (A) Diagram of Nudel and its mutants used in this work. Numbers indicate positions of amino acid residues. (B) Association of Nudel or mutants with other cellular proteins. FLAG-tagged Nudel or mutants were expressed in HEK293T cells and subjected to coimmunoprecipitation using anti-FLAG M2 resin. Cells transfected with the vector served as a control. Antibodies against the indicated proteins were used for immunoblotting (lanes 6–10). Protein levels in each cell lysate are also shown (lanes 1–5). (C) Nudel^{N20} is able to dimerize. GFP-Nudel^{P2N} was coexpressed with FLAG-Nudel or Nudel^{N20} transiently in HEK293T cells (lanes 1 and 2). Control cells expressed only GFP-Nudel^{P2N} but were cotransfected with the vector pUHD30F (lane 3). After coimmunoprecipitation with anti-FLAG M2 resin (lanes 4–6), samples were immunoblotted with either anti-FLAG mAb (top) or anti-GFP antibody (bottom). The slower migrating form of Nudel^{N20} was probably due to phosphorylation (Yan et al., 2003).

which might be other tubulin isoforms. All of these proteins except Lis1 were in complex with Nudel^{N20} (Fig. 1 B, lane 8), whereas basically only Lis1 bound to Nudel^{C36} strongly (Fig. 1 B, lane 9). FLAG-Nudel$^{N20/C36}$ showed little, if any, association with these proteins (Fig. 1 B, lane 10), suggesting that it might serve as a nonfunctional negative control.

Because Nudel homodimerizes through its NH_2-terminal coiled coil domain in yeast two-hybrid assays (Sasaki et al., 2000), we examined if Nudel^{N20} retained this property. As shown in Fig. 1 C, both FLAG-Nudel (lane 4) and Nudel^{N20} (lane 5) pulled down GFP-Nudel^{P2N}, a mutant containing the NH_2-terminal 201 amino acids, indicating that Nudel^{N20} was still able to homodimerize. Thus, its phenotypes would be mainly attributed to loss of Lis1 association.

Involvement of Nudel in membrane trafficking

Cytoplasmic dynein is essential for proper positioning of many membranous organelles in the vicinity of centrosomes

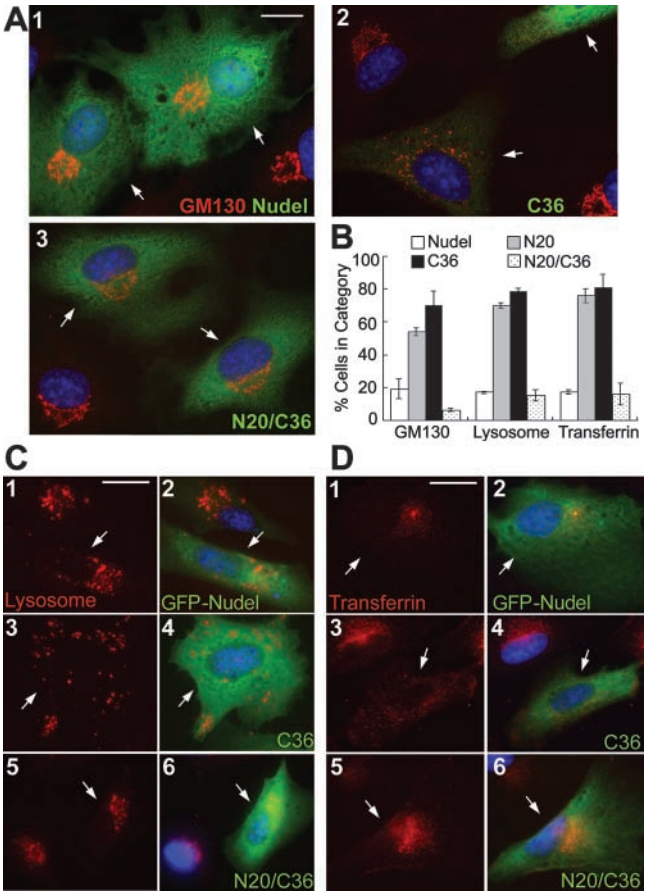

Figure 2. **Fragmentation/dispersion of the cis-Golgi cisternae, lysosomes, and endosomes by mutant Nudel.** (A, C, and D) CV1 cells transiently expressing Nudel or mutants (green) were processed to show nuclear DNA (blue) and different membrane organelles (red). Transfectants are indicated by arrows. (A) The cis-Golgi cisternae, which was decorated with anti-GM130 antibody (red) after fixation in methanol. FLAG-Nudel isoforms were labeled with anti-FLAG mAb (green). Bar, 15 μm. (B) Statistic results (mean ± SD) showing severity of vesicle dispersion. $n = 300$, two experiments. (C and D) Lysosomes and transferrin receptor-containing endosomes (red). Vesicles were labeled in living cells before fixation in PFA. GFP-Nudel or mutants were expressed to facilitate identification of the transfectants. Bars, 20 μm.

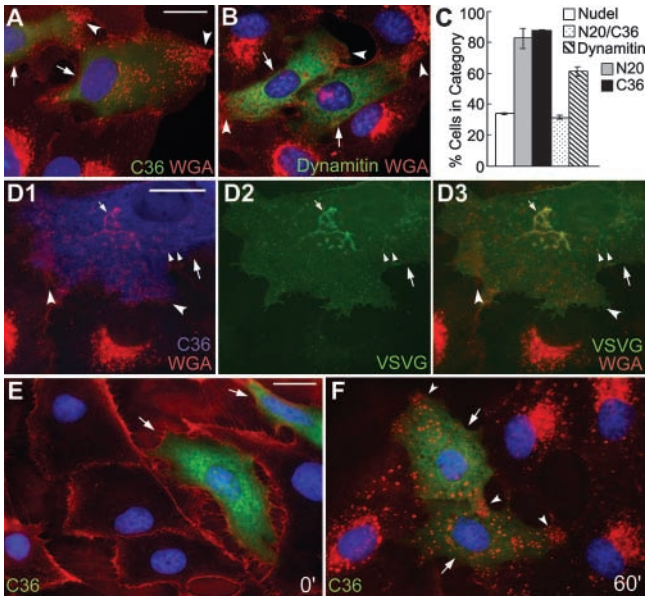

Figure 3. **Peripheral distribution of endosomes containing WGA-binding sites by Nudel mutant or dynamitin in CV1 cells.** (A, B, and D–F) Large arrows indicate transfectants and concave arrowheads indicate vesicles accumulated at the cell processes. Bars, 20 μm. (A and B) Cells expressing FLAG-tagged Nudel^{C36} or dynamitin were fixed in methanol and labeled with TRITC-WGA (red), anti-FLAG mAb (green), and DAPI (blue). (C) Statistic results (mean ± SD) showing severity of vesicle dispersion. $n = 300$, three experiments. (D) Distributions of VSVG-GFP (green) and WGA-positive vesicles (red) in a typical FLAG-Nudel^{C36} expressor (blue). Small arrows and arrowheads indicate the Golgi cisternae and typical secretory vesicles, respectively. (E and F) Binding of WGA (red) to the plasma membrane at 4°C and its endocytosis into GFP-Nudel^{C36} expressors (green) after 60 min at 37°C.

in a MT-dependent way. Disruption of dynein activity by antibody microinjection, targeted disruption, or overexpression of dynamitin to displace dynein from its cargoes leads to dispersion/fragmentation of the Golgi cisternae, lysosomes, endosomes, and ERGIC throughout the cytoplasm due to impairment of minus end–directed motions (Burkhardt et al., 1997; Harada et al., 1998). Thus, we examined whether mutant Nudel affected distributions of the membrane organelles in CV1 cells.

We initially examined the cis-Golgi cisternae decorated by anti-GM130 antibody (Lowe et al., 1998). Its perinuclear clustering was not affected in the majority of FLAG-Nudel expressors (Fig. 2 A, 1; and Fig. 2 B). In contrast, severe fragmentation and dispersion of the Golgi apparatus were observed upon expression of the mutant defective in binding to either Lis1 or DHC (Fig. 2 A, 2; Fig. 2 B; and not depicted). The extent of Golgi fragmentation strongly correlated with expression levels, with the DHC-binding defective mutant as the most potent because the threshold to cause Golgi fragmentation was relatively low and the cisternae were frequently scattered widely in the cytoplasm (Fig. 2 A, 2; and not depicted). Considering a background of ~3% in surrounding untransfected cells, Nudel$^{N20/C36}$ had little effect (Fig. 2 A, 3; and Fig. 2 B). Similar effects were observed for lysosomes (Fig. 2, B and C), endosomes formed by transferrin receptor-mediated uptake (Fig. 2, B and D) or by fluid phase uptake of Texas red–labeled dextran (not depicted).

When the trans-Golgi cisternae and endosomes containing WGA-binding sites (Virtanen et al., 1980; Raub et al., 1990) were examined, a substantial amount of the WGA-positive vesicles was aligned at the cell processes in what appeared to be parallel arrays in cells expressing the mutant incapable of binding to either Lis1 or DHC (Fig. 3 A and not depicted). In comparison, dynamitin overexpression also resulted in very similar phenotypes (Fig. 3 B; Burkhardt et al., 1997) with lower efficacy on vesicle dispersion (Fig. 3 C). To understand the nature of the peripheral vesicles, a secretory protein marker, VSVG-GFP (Presley et al., 1997), was coexpressed with the DHC-binding defective mutant, Nudel^{C36} (Fig. 3 D). Lack of its colocalization with the peripheral vesicles suggested that the latter did not belong to the secretory pathway but might be endo-

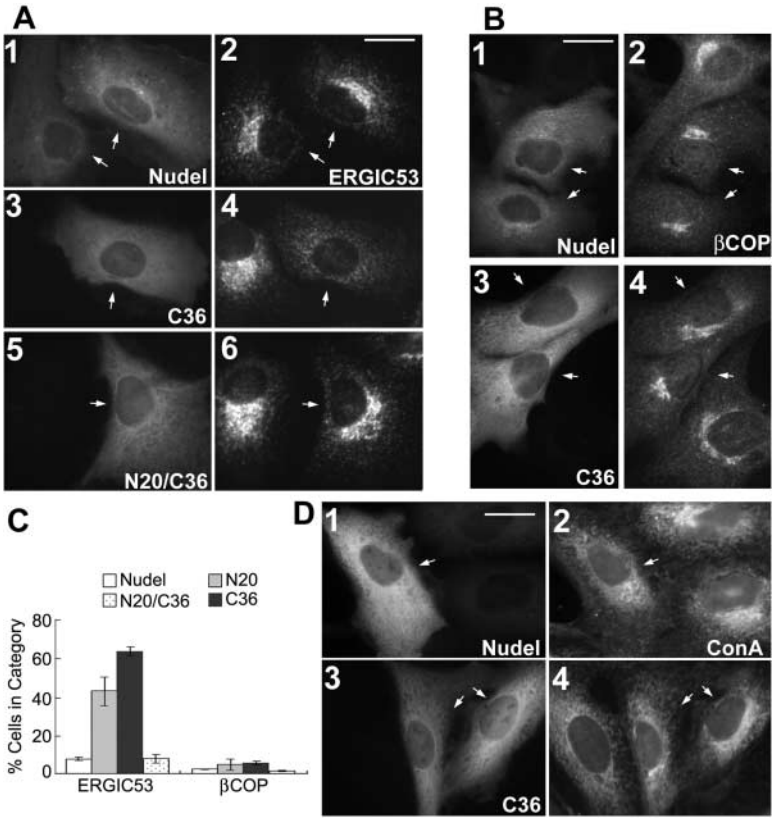

Figure 4. **Distributions of the ERGIC, COPI-coated compartments, and ER.** CV1 cells expressing GFP-tagged (A and B) or FLAG-tagged (D) Nudel isoforms are indicated by arrows. Bars, 20 μm. (A and B) Cells were labeled for the ERGIC with anti-ERGIC53 mAb or COPI-coated vesicles with anti-βCOP mAb. (C) Statistic results (mean ± SD) showing severity of vesicle dispersion. $n = 300$, two experiments. (D) Cells were labeled for the ER with Texas red–conjugated Con A.

somes (Fig. 3 D, D3). The speculation was confirmed by endocytic assays in which endocytosis was first blocked at 4°C to leave WGA at plasma membranes (Fig. 3 E), and then facilitated by shifting back to 37°C (Raub et al., 1990). After 60 min, the endosomes were transported to perinuclear regions in GFP-Nudel expressors (not depicted) and untransfected cells (Fig. 3 F), but not in Nudel^{C36} expressors (Fig. 3 F). Instead, they were dispersed, with clear accumulation at the cell processes (Fig. 3 F).

Perinuclear accumulation of the ERGIC was also disrupted when the mutant Nudel, incapable of binding to either Lis1 or DHC, was expressed (Fig. 4, A and C; and not depicted). However, when COPI-coated vesicles were examined using an antibody to βCOP, a COPI subunit (Lippincott-Schwartz et al., 1995), their clustering was not abolished in transfectants, despite some reduction in the size of βCOP-positive compartments (Fig. 4, B–C; and not depicted). Such a finding was in agreement with the idea that COPI vesicles, which recycle proteins from the cis-Golgi cisternae back to the ER, are transported mainly by the plus end–directed motor, kinesin (Lippincott-Schwartz et al., 1995). Similarly, distributions of the ER were also not affected (Fig. 4 D and not depicted; Feiguin et al., 1994; Burkhardt et al., 1997).

Impairment of the minus end–directed motility by mutant Nudel

The ordered alignment of peripheral endosomes (Fig. 3 A) implied their association with cell skeletons, possibly MTs. Thus, we tested this using MT regrowth assays. Nocodazole treatment (5 μg/ml) for 3 h completely disassembled MTs (not depicted) and resulted in fragmentation/dispersion of WGA-positive organelles (Fig. 5, A and B, A1 and B1, respectively). Removal of the drug for 1 h allowed perinuclear clustering of the endosomes in control cells (Fig. 5, A and B, A2 and B2, respectively). In contrast, although abolished by nocodazole, the peripheral accumulation of endosomes was reestablished in cells expressing the mutant lacking interaction with Lis1 or dynein after removal of the drug (Fig. 5 B and not depicted). These results suggest that the peripheral endosomes are capable of the plus end–directed but not the minus end–directed motions along MTs.

To further corroborate the observations, we monitored lysosome trafficking in living cells by time-lapse microscopy. In GFP-Nudel expressors or untransfected cells, the majority of lysosomes swirled randomly and slowly in a given time window, whereas the rest exhibited rapid movement in mainly inward and outward directions (Video 1, available at http://www.jcb.org/cgi/content/full/jcb.200308058/DC1; Matteoni and Kreis, 1987). Moving lysosomes frequently paused halfway and resumed motions in the same or opposite direction. However, the net displacements were usually centripetal (Fig. 5 C and Video 1). Nocodazole treatment abolished such movement (unpublished data), indicative of MT-based motility (Matteoni and Kreis, 1987). However, upon expression of GFP-Nudel^{C36}, the directional lysosome trafficking was significantly inhibited. Moreover, the outward motions predominated, correlating with obvious peripheral accumulation of lysosomes (Fig. 5 D and Video 2, available at http://www.jcb.org/cgi/content/full/jcb.200308058/DC1).

Detailed analysis was performed manually. In the 2-min windows of monitoring, 113 lysosomes exhibited directional

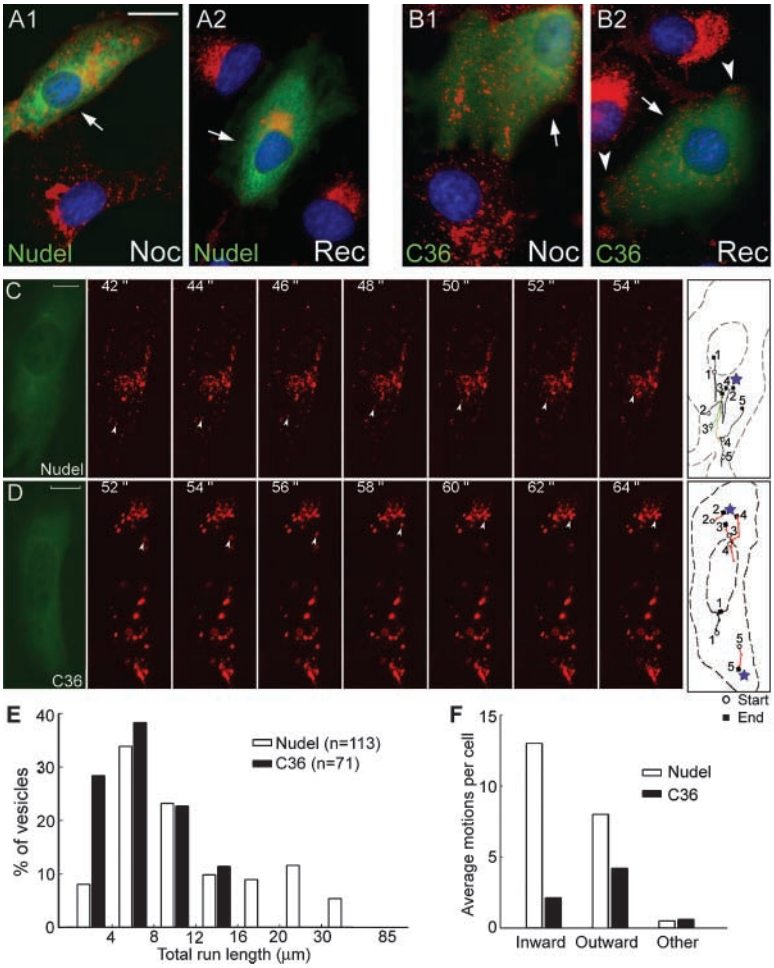

Figure 5. **Impairment of inward vesicle trafficking by the DHC-binding defective Nudel mutant.** (A and B) Redistributions of WGA-positive vesicles (red) after nocodazole treatment (Noc) or after recovery from the treatment for 1 h (Rec). CV1 cells expressing Nudel or Nudel^{C36} (green) are indicated by arrows. The trans-Golgi cisternae/endosomes (red) and nuclear DNA (blue) were labeled with TRITC-WGA and DAPI. Arrowheads indicate vesicles accumulated at the cell processes. Bar, 20 μm. (C and D) Time-lapse microscopy. Living CV1 cells expressing GFP-Nudel or Nudel^{C36} were labeled for lysosomes with LysoTracker and recorded live every 2 s for 120-s consecutive frames showing directional movement of a typical lysosome (arrowheads) and are presented for each type of transfectant. The first and last frames show the GFP fluorescence and tracks of five lysosomes with the longest run lengths, respectively. Red tracks refer to motions with net outward displacements. Where lysosomes cluster is labeled by a star. Track 3 in C corresponds to the indicated inwardly moving lysosome, whereas track 4 in D corresponds to the outwardly moving one. Complete sets of images are available as supplemental material (Videos 1 and 2, available at http://www.jcb.org/cgi/content/full/jcb.200308058/DC1). Bars, 10 μm. (E) Distributions of lysosomes with indicated ranges of total run lengths. (F) Average events of directional motions per cell. See Materials and methods for definitions.

motions in 10 GFP-Nudel expressors (average 11.3 lysosomes per cell), whereas 71 were found in 15 cells expressing the mutant lacking DHC binding (average 4.7 per cell). In the mutant expressors, all the lysosomes had total run lengths (track lengths) shorter than 16 μm (minimal 1.4 μm, maximal 15.5 μm; Fig. 5 E). In contrast, 25.7% lysosomes with directional motions traveled longer than 16 μm (minimal 2.7 μm, maximal 84.9 μm) in GFP-Nudel expressors (Fig. 5 E). Such a difference was mainly due to lack of minus end–directed movement because the average inward motion events in a mutant expressor were 6.1-fold lower than in a wild-type expressor, compared with only 1.9-fold decrease in the average outward motion events per cell (Fig. 5 F and Videos 1 and 2). Consistently, the velocities of inward motions in the mutant expressors were lower than 1.2 μm/s, whereas 20.0% of those in wild-type expressors moved faster than that (maximal 2.7 μm/s; Fig. S1 A, available at http://www.jcb.org/cgi/content/full/jcb.200308058/DC1). Conversely, although lysosomes in wild-type expressors tended to move faster outwardly (Fig. S1 B), the difference was not as significant compared with that for inward motions. Similarly, the difference in the duration time of continual movements was also less apparent for either moving directions (Fig. S1, C and D). Together, the major defects in the mutant expressors were considerable reductions in both the frequencies and velocities of the minus end–directed motions.

Reduction of protein secretion by mutant Nudel

What would be the collective outcomes when both organizations and traffic of multiple membrane organelles were compromised by mutant Nudel? To partially address this question, we examined the effect on protein secretion using human placental lactogen (hPL; Walker et al., 1991) tagged with GFP at the COOH terminus as a marker. Secretion of hPL-GFP was confirmed through its detection in the medium (Fig. 6 A). Microscopic examinations indicated that the protein in the medium was not a result of cell death (unpublished data). For comparable results, we used the tetracycline (Tet)-responsive promotor (Gossen and Bujard, 1992) to control the expression of FLAG-Nudel and mutants (Fig. 6 B). Immunofluorescence staining indicated that over 90% of FLAG-positive cells coexpressed hPL-GFP in cultures lacking Tet, whereas only a few FLAG-positive cells were noticed in cultures with Tet (unpublished data).

As shown in Fig. 6 D, the secreted protein was readily detected in medium cultured for 12 h or longer. Expression of FLAG-Nudel did not significantly alter the secretion rate of hPL-GFP. The secreted hPL-GFP at 24 h (103 ± 15%) was comparable to that (100%) in the corresponding Tet$^+$ sample. The double deletion mutant Nudel$^{N20/C36}$ had mild effects on the secretion (88 ± 5%), whereas both the Lis1-binding defective mutant Nudel^{N20} and the DHC-binding defective mutant Nudel^{C36} showed strong inhibition, reducing hPL levels to 46 ± 19% and 21 ± 6%, respectively (Fig. 6 E).

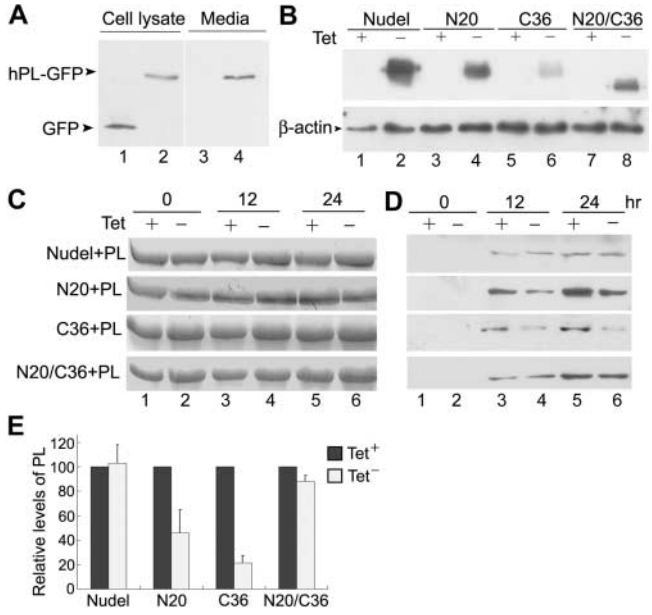

Figure 6. **Inhibition of constitutive protein secretion by mutant Nudel.** (A) Secretion of hPL-GFP, but not GFP, from HEK293T cells. (B) Controlled expression of Nudel by tetracycline (Tet). To examine the effects of FLAG-Nudel isoforms on hPL-GFP secretion, HEK293T cells were transfected and cultured in the presence (+) or absence (−) of Tet as described in Materials and methods. At the end of the assays, cell lysates were subjected to immunoblotting using anti-FLAG mAb (top), while β-actin served as a loading control (bottom). (C) BSA as the loading control of culture media. 5 μl of each medium collected at the indicated time points was subjected to Coomassie blue staining after SDS-PAGE. (D) Secretion levels of hPL-GFP. 10 μl of each medium was immunoblotted using anti-GFP antibody. (E) The relative secretion levels at 24 h were quantified for comparison. The relative secretion levels in Tet^- samples are normalized to that of corresponding Tet^+ samples (i.e., 100) and presented as the mean ± SD.

Dispersion of the Golgi cisternae upon silencing of Nudel expression

To further corroborate a role of Nudel in membrane traffic, we knocked down its expression through RNA interference (RNAi). Liposome transfection of small interference RNA (SiRNA) for Nudel into HEK293T cells with pEGFP-F to express a membrane-associated GFP marker resistant to methanol fixation (Jiang and Hunter, 1998) resulted in extensive cell death. In a typical set of experiments, when 10 random areas were examined 3 d after transfection, only ~11.8% transfectants survived compared with those transfected with pEGFP-F alone. Immunoblotting indicated a 37% decrease of Nudel level compared with control cells (Fig. 7 A), which was informative but might not reflect the real situation because most cells with insufficient Nudel might be inviable and excluded from the sample. In fact, a more dramatic repression was achieved when exogenous Nudel was examined. In the presence of the SiRNA, GFP-Nudel level was only 2.3% of the control (Fig. 7 B, lanes 1 and 2; and Fig. 7 C, 1–6). In comparison, the SiRNA resulted in a 45% reduction for GFP-NudE (Fig. 7 B, lanes 3 and 4; and Fig. 7 C, 7–9), which shares a 53% identity with Nudel (Yan et al., 2003), with little effects on β-actin, GFP, and red fluorescence protein DsRed (Fig. 7, A–C). Moreover, despite the low levels of GFP-Nudel in the presence of the SiRNA, cell death was not obvious. Approximately 87% of transfectants survived, probably due to maintenance of critical Nudel levels by the trace amount of GFP-Nudel (Fig. 7 B, lane 2). Together, we attributed the cell death phenotype to repressed Nudel expression but not to toxicity of the SiRNA preparations. Therefore, the Nu-

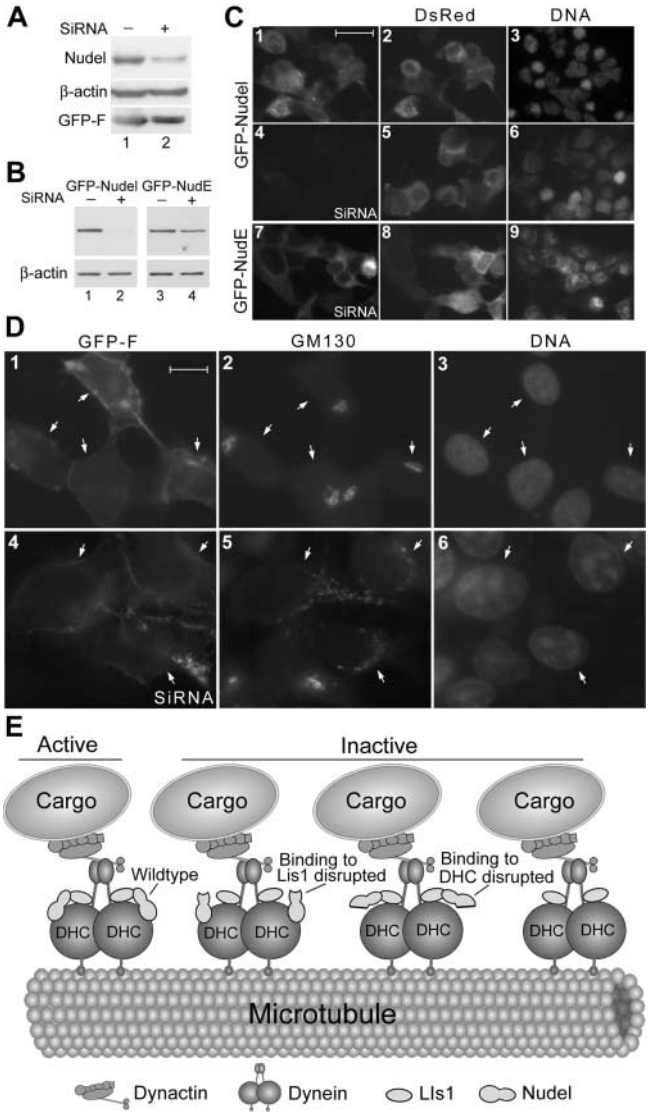

Figure 7. **Golgi fragmentation upon silencing of Nudel in HEK293T cells and a model for Nudel functions in dynein motor activity.** (A) Repressed expression of endogenous Nudel by SiRNA. GFP-F, a membrane-associated GFP variant, served as a transfection marker. (B and C) The SiRNA specifically repressed GFP-Nudel expression. (B) The top panels were immunoblotted using anti-GFP antibody. (C) The red fluorescence protein (DsRed) served as a transfection marker. Bar, 50 μm. (D) Effects of Nudel SiRNA on cis-Golgi organization. Cells transfected as in A were labeled with anti-GM130 antibody to decorate the cis-Golgi cisternae. Arrows indicate GFP-F expressors. Bar, 20 μm. (E) A model summarizing the results. We propose that active dynein motor requires Nudel and its interactions with both Lis1 and DHC. Disrupting either interaction or silencing Nudel expression impairs dynein motor activity. Disrupting both interactions inactivate Nudel, thus generating a null mutant. Homodimerization of Lis1 and Nudel (Sasaki et al., 2000) is not considered. Therefore, the actual situations must be more intricate. Existence of NudE further complicates the situation.

del SiRNA was highly efficient and specific. Interestingly, expression of GFP-NudE in the presence of Nudel SiRNA (Fig. 7 C, 7–9) also prevented cells from extensive death. 72% of transfectants survived.

Upon transfection of Nudel SiRNA, 56.9 ± 2% of cells (n = at least 100, three experiments) positive for GFP-F exhibited dispersed GM130 staining (Fig. 7 D, 4–6). The Golgi fragmentation was not due to cell death because most cells with such phenotypes still possessed normal cell shape and nuclei. Only 6.9 ± 2.9% of cells transfected with pEGFP-F alone had abnormal Golgi morphology, the rest of the cells showed tight clustering of GM130 staining (Fig. 7 D, 1–3). In fact, in samples transfected with Nudel SiRNA, even cells without clear GFP-F expression exhibited varying extents of Golgi fragmentation (unpublished data), possibly due to uptake of only SiRNA because its molar ratio to pEGFP-F was >200:1.

Discussion

This work elucidates a role of Nudel in membrane traffic. Fragmentations/dispersions of the Golgi cisternae, ERGIC, lysosomes, and endosomes by mutants lacking association with Lis1 (i.e., Nudel^{N20}) or DHC (i.e., Nudel^{C36}) implicate Nudel in MT minus end–directed membrane transport (Figs. 2–5). Such a conclusion is further corroborated with the RNAi experiments (Fig. 7). Nudel^{C36} is generally more potent, coincident with its failure to precipitate multiple proteins relevant to dynein functions (Fig. 1). Consistently, associations of Nudel with the ER/Golgi membrane, synaptosomal membrane, and synaptic vesicle-enriched fractions from brain cells are documented (Niethammer et al., 2000). Nudel also associated with endomembrane fraction from HEK293T cells, a property appearing to require both the Lis1 and dynein-binding domains (unpublished data). Because overexpression of the wild-type Nudel or the mutant capable of binding to neither Lis1 nor DHC (i.e., Nudel$^{N20/C36}$) exhibited much less effect on organelle distributions, we attribute their influences to weak dominant-negative effects and/or artifacts of overexpression, and thus consider them as negative controls. Therefore, our results specify that Nudel functions in membrane trafficking rely largely on the integrity of both the Lis1 and dynein-binding domains, supporting the idea that interplays of the three partners are critical for dynein motor activity (Sasaki et al., 2000; Wynshaw-Boris and Gambello, 2001; Gupta et al., 2002; Yan et al., 2003).

Several lines of evidence collectively indicate that Nudel functions in endomembrane flux through cytoplasmic dynein. First, a mutant incapable of direct interaction with DHC (Fig. 1; Sasaki et al., 2000) causes dispersions of the aforementioned organelles whose perinuclear distributions require dynein-mediated transport (Figs. 2–4). The phenotypes closely resemble those when dynein functions are inactivated by other means (Burkhardt et al., 1997; Harada et al., 1998; Valetti et al., 1999). In fact, the phenotypes for WGA-positive vesicles caused by overexpression of either dynamitin or the DHC-binding defective Nudel mutant are basically indistinguishable (Fig. 3). Moreover, selective disruption of Nudel's interaction with Lis1, another dynein partner, also leads to similar but slightly milder phenotypes (Fig. 1 and not depicted). However, organelles such as the ER and COPI-coated vesicles, whose maintenance and traffic do not entirely depend on dynein (Lippincott-Schwartz et al., 1995; Burkhardt et al., 1997), are not significantly affected by these mutants.

Second, time-lapse microscopy reveals clear defects in minus end–directed motions of lysosomes in living cells expressing the DHC-binding defective Nudel mutant (Fig. 5). Both the frequencies and velocities of inward trafficking are considerably reduced compared with those in the wild-type expressors. Despite similar tendencies for outward motilities, the differences are not as significant. We also confirmed that the radial MT arrays were not disrupted in transfectants (unpublished data). Therefore, dispersions of the membrane organelles and the lack of inward motions were not due to loss of MT focus at the MT-organizing center.

Finally, fragmentation of the Golgi apparatus after knocking down Nudel expression by RNAi further indicates requirement of Nudel for dynein function (Fig. 7). Moreover, the extensive cell death after repression of endogenous Nudel by RNAi and the rescue by exogenous protein also highlight its importance, like Lis1 (Hirotsune et al., 1998), for cell survival. Such properties may at least partially reflect critical roles of cytoplasmic dynein in trafficking, mitosis, and cell migration. In addition, several previous works suggest NudE as a functional paralogue of Nudel (Feng et al., 2000; Sasaki et al., 2000; Yan et al., 2003). Consistently, inhibition of NudE by RNAi also exhibited similar cell death and conferred the Golgi fragmentation in 59.2 ± 6.9% HEK293T cells (unpublished data). Prevention of Nudel SiRNA-induced cell death by overexpressing GFP-NudE also suggests a complementary effect. Therefore, Nudel, NudE, and Lis1 serve as regulators for a variety of dynein functions.

Three factors, the motor–cargo association, motor–MT interaction, and motor activity, dictate cargo motilities directed by MT-based motors. Neither the Lis1- nor the DHC-binding defective mutants attenuate the membrane associations of dynactin/dynein (unpublished data). In the time-lapse experiments, the similar durations for inward motions in the wild-type Nudel, or the mutant expressors (Fig. S1), suggest roughly intact dynein–cargo and dynein–MT interactions. Consistently, in mitotic cells, blocking the dynein-mediated transport of kinetochore proteins to spindle poles by these mutants does not disrupt localizations of dynein and its cargo proteins on the spindle, also suggesting undisrupted dynein–cargo and dynein–MT interactions (Yan et al., 2003; Yang et al., 2003; unpublished data). Together, the reduced velocities and frequencies of the inward lysosome trafficking (Fig. 5) are mainly attributed to impaired dynein motor activity by the DHC-binding defective mutant. In contrast, kinesin activity appears fairly maintained. The moderately decreased outward motilities (Fig. 5 F and Fig. S1) may be due to improbability for peripheral lysosomes to further move outwardly without preceding inward traffic. Therefore, it is concluded that the Nudel mutants mainly impair dynein motor activity by selectively abolishing either the Nudel–Lis1 or the Nudel–DHC interaction (Fig.7 E). Moreover, the double mutant lacking interaction with both Lis1 and DHC was basically null, indicating that the remaining regions of Nudel, e.g., the

dimerization domain (Fig. 1; Sasaki et al., 2000), have little effect in regulating dynein motor (Fig. 7 E). In comparison with Nudel, phenotypes by dynamitin overexpression are due to dissociation of dynein from the dynactin complex, and thus from its cargos (Burkhardt et al., 1997). Nudel also functionally differs from the Rab family of small GTPase, which regulates dynein-mediated membrane traffic by recruiting the dynein–dynactin complex to appropriate membrane organelles (Jordens et al., 2001; Matanis et al., 2002).

Inhibition of hPL-GFP secretion by mutant Nudel (Fig. 6) may be delineated as a collective result of multiple defects. On the one hand because MT disassembly by nocodazole does not abolish protein secretion but only diminishes the secretion rate of a similar protein marker (Wacker et al., 1997); MT-based motors appear just as important for the efficiencies of membrane trafficking. Similarly, lack of retrograde transport and perinuclear distributions of many organelles in the secretory pathway through inactivation of dynein may contribute to the reduced rates of protein secretion. On the other hand, because many factors need to be recycled back to the previous organelles during membrane trafficking (Lippincott-Schwartz et al., 1989; Mallet and Maxfield, 1999; Matanis et al., 2002), interruption of such processes by impairing dynein activity may also indirectly affect secretion.

Materials and methods

Plasmid constructs

pUHDF-Nudel is a plasmid for expression of FLAG-tagged full-length Nudel under control of the Tet-responsive promoter (Gossen and Bujard, 1992; Yan et al., 2003). All the deletion mutants of Nudel were made by PCR. pEGFP-C1 (CLONTECH Laboratories, Inc.) was used to express GFP-tagged Nudel and NudE. The full-length cDNA for hPL, also called chorionic somatomammotropin (Walker et al., 1991), was amplified by PCR from a placenta cDNA library (CLONTECH Laboratories, Inc.) and cloned into pCD-GFP (a gift from G. Pei, Chinese Academy of Sciences, Shanghai, China; Wang et al., 2000) to constitutively express hPL-GFP. The plasmid for expressing VSVG-GFP (Presley et al., 1997) was provided by J. Lippincott-Schwartz (National Institute of Child Health and Human Development, National Institutes of Health, Bethesda, MD). Dynamitin cDNA was amplified by reverse transcription PCR from HEK293T cells and cloned into pUHD30F (Zhu, 1999). DNA fragments obtained by PCR were confirmed by sequencing.

Cell culture and transfection

Monkey kidney CV1 and human embryonic kidney HEK293T cells were grown in DME (GIBCO BRL) supplemented with 10% calf serum (Sijiqing Company) in an atmosphere containing 5% CO_2. Transfection was performed using calcium phosphate method unless otherwise indicated. Generally, HEK293T was used for biochemical studies due to high transfection efficiencies of up to ~80%, whereas CV1 was used for cytological experiments because it is a normal cell line with larger cell sizes and better attachment to coverslips to allow easier examinations on vesicle distributions. Both cell lines express Nudel (Fig. 7; Yan et al., 2003).

Antibodies and staining reagents

Anti-FLAG M2, anti-DIC, anti-βCOP, anti–α-tubulin, and anti–γ-tubulin mAbs, TRITC-WGA, and Texas red–labeled Con A were purchased from Sigma-Aldrich. Antidynamitin mAb was obtained from BD Biosciences. Polyclonal anti-DHC and anti-Lis1 antibodies were obtained from Santa Cruz Biotechnology, Inc. Lysotracker red (provided by M. Zhao, Chinese Academy of Sciences, Shanghai, China), Texas red–conjugated transferrin, and dextran were from Molecular Probes. Secondary antibodies labeled with FITC, TRITC, or Cy5 were purchased from Pierce Chemical Co. or Rockland. Antibodies to ERGIC53, GM130, or Nudel were provided by H.-P. Hauri (University of Basel, Basel, Switzerland), M. Lowe (University of Manchester, Manchester, UK), and L.-H. Tsai (Harvard Medical School, Boston, MA), respectively.

Coimmunoprecipitation and immunoblotting

Transfected HEK293T cells were collected and washed twice with PBS. Coimmunoprecipitation using anti-FLAG M2 affinity resin (Sigma-Aldrich) was performed as described previously (Yan et al., 2003). Blots were developed in Renaissance ECL reagent (NEN Life Science Products) and exposed to X-ray films (Kodak). Band intensities were quantitated using Adobe Photoshop 6.0 (Yan et al., 2003). Data were presented as the mean ± SD.

Uptake of endocytic tracers

For tracing receptor-mediated endocytosis, CV1 cells were incubated with 20 μg/ml of Texas red transferrin or with dextran for 30 min at 37°C before immediate fixation with 4% PFA at 37°C for 15 min (Kauppi et al., 2002). To analyze the endocytic traffic of WGA-binding sites in plasma membranes, CV1 cells were incubated with 10 μg/ml TRITC-conjugated WGA in PBS for 30 min at 4°C, rinsed, and cultured in serum-free medium at 37°C (Raub et al., 1990). Samples were fixed at 0 and 60 min with PFA.

Fluorescence staining and microscopy

Cells grown on sterile coverslips were fixed in cold methanol or 4% PFA before indirect immunofluorescence staining using appropriate antibodies. Nuclear DNA was stained with DAPI. The cis-Golgi cisternae, trans-Golgi cisternae, or ER was decorated with anti-GM130 antibody (Lowe et al., 1998), TRITC-WGA (Virtanen et al., 1980), or Texas red–labeled Con A (Virtanen et al., 1980). The ERGIC was labeled with anti-ERGIC53 mAb (Hauri et al., 2000), whereas COPI vesicles were labeled with anti-βCOP mAb. Lysosomes were stained with LysoTracker red (Molecular Probes) at a concentration of 50 nM in living cells followed by three times of wash before time-lapse microscopy or fixation in 4% PFA. Cells with clearly dispersed organelles were scored in a blind fashion independently by three researchers with results averaged. Percentages of affected cells were presented as the mean ± SD from two to three independent experiments. Images were captured using a cooled CCD SPOT II (Diagnostic Instruments) on a microscope (model BX51; Olympus) with UPlanApo 100×/1.35 Oil Iris and UPlanFL 60×/1.25 Oil Iris objectives, except that those stained with cy5-conjugated secondary antibodies (Fig. 3 D) were captured using a CCD camera (model DC350F; Leica) on a microscope (model DM5000B; Leica). Grayscale images (1,315 × 1,033 pixels) were recorded and converted to color using Confocal Assistant 4.02 when required. Illustrations were organized using Photoshop. Sometimes, nonlinear adjustment was applied to DAPI staining for optimal indication of nuclear positions.

Time-lapse microscopy was performed at 37°C using a LUMPlanFL 60×/0.9 water immersion objective. Images were recorded at 2-s intervals including exposure time for 2 min and processed using an NIH image program and Quick-time v5.02. Vesicle movement was defined as "directional" when the direction was fixed in three or more consecutive frames with the run length (track length) between two adjacent frames longer than 0.7 μm (equivalent to 4 pixels in images), otherwise it was considered "random." The directions were further classified as "inward" or "outward" for movement toward or away from the nucleus, or "other" if difficult to define. For track display, coordinates of individual vesicles in each frame were measured using the image program, stored in Microsoft Excel, and converted to tracks using SigmaPlot. The tracks were superimposed onto an outline of the cell drawn according to its differential interference contrast image. The run length of each directional motion was the track length from the start position to the next pause position. The velocity for each directional movement was an average obtained by dividing the run length by the duration time. The total run length of a vesicle was defined as the sum of all its run lengths regardless of direction and succession.

Secretion assays

HEK293T cells were cotransfected with pCD-hPL-GFP, pUHDF-Nudel, or a mutant and p15-1 at a molar ratio of 1:4:4 for 24 h in the presence of 1 μg/ml Tet (Gossen and Bujard, 1992). After three times of gentle wash, cells were split equally into two 60-mm dishes to guarantee minimal variations in cell numbers and transfection efficiencies. One plate was cultured in the presence of Tet, whereas the other was cultured without Tet. A glass coverslip was placed in each dish. After an additional 12 h of incubation, old culture media were removed and 2 ml of corresponding fresh media was added. 30 μl of each medium was collected at 0, 12, and 24 h. At the end of the experiment, cells were collected for immunoblotting. The coverslips were fixed in methanol and stained with anti-FLAG mAb to evaluate the quality of induction and cotransfection efficiencies. For quantitation, hPL-GFP intensities in each pair of samples at 24 h were normalized to corresponding BSA levels. Relative secretion levels were calculated by setting the level in the Tet^+ sample as 100. Results were averaged from two experiments and presented as the mean ± SD.

SiRNA preparation and transfection

Nudel and NudE SiRNA were prepared using Genesilencer kit following the manufacturer's protocols (Gene Therapy Systems). In brief, the first 500 bp of Nudel or NudE cDNA from the start codon was transcribed in vitro into double stranded RNA using T7 RNA polymerase followed by cleavage with Dicer enzyme (Myers et al., 2003) for 24 h and column purification. Transfection of SiRNA was performed in 12-well plates with Lipofectamine2000 (Life Technologies) as described by the manufacturer for adherent cell lines. 0.1 μg pGFP-Nudel or pGFP-NudE, 0.4 μg DsRed plasmid, and 0.12 μg SiRNA formulated into liposomes were applied per well. Cells were processed 48 h after transfection for immunoblotting and 48, 72, and 96 h after transfection for fluorescence microscopy. To repress the endogenous protein, 0.1–0.3 μg SiRNA and 0.1 μg pEGFP-F (CLONTECH Laboratories, Inc.; Jiang and Hunter, 1998) were transfected per well. Cells were processed 72 h after transfection.

Online supplemental material

Quicktime movies (six frames per second) show lysosome motilities in typical CV1 cells expressing GFP-Nudel (Video 1, frame 1) or GFP-Nudel^{C36} (Video 2, frame 1). The tracks of five lysosomes with the longest run lengths in each cell are displayed in the last frame. Red tracks refer to motions with net outward displacements. Representative frames in Videos 1 and 2 are displayed in Fig. 5 (C and D) to show movement of typical vesicles. Detailed analysis is shown in Fig. 5 (E and F) and Fig. S1. Online supplemental material is available at http://www.jcb.org/cgi/content/full/jcb.200308058/DC1.

We are particularly grateful to Drs. H.-P. Hauri, L.-H. Tsai, and M. Lowe for antibodies to ERGIC53, Nudel, and GM130, respectively; J. Lippincott-Schwartz for VSVG-GFP plasmid; G. Pei for pCD-GFP; and M. Zhao for Lysotracker red.

This work was supported by grants 30025021, 30330330, and 39970160 from the National Science Foundation of China, grant KSCX2-2-02 from the Chinese Academy of Sciences, and grant 2002CB713802 (The National Key Basic Research and Development Plan) from the Ministry of Science and Technology of China.

Submitted: 11 August 2003
Accepted: 14 January 2004

References

Brunet, S., and I. Vernos. 2001. Chromosome motors on the move. From motion to spindle checkpoint activity. *EMBO Rep.* 2:669–673.

Burkhardt, J.K., C.J. Echeverri, T. Nilsson, and R.B. Vallee. 1997. Overexpression of the dynamitin (p50) subunit of the dynactin complex disrupts dynein-dependent maintenance of member organelle distribution. *J. Cell Biol.* 139: 469–484.

Efimov, V.P., and N.R. Morris. 2000. The LIS1-related NUDF protein of *Aspergillus nidulans* interacts with the coiled-coil domain of the NUDE/RO11 protein. *J. Cell Biol.* 150:681–688.

Feiguin, F., A. Ferreira, K.S. Kosik, and A. Caceres. 1994. Kinesin-mediated organelle translocation revealed by specific cellular manipulations. *J. Cell Biol.* 127:1021–1039.

Feng, Y., E.C. Olson, P.T. Stukenberg, L.A. Flanagan, M.W. Kirschner, and C.A. Walsh. 2000. LIS1 regulates CNS lamination by interaction with mNudE, a central component of the centrosome. *Neuron.* 28:665–679.

Gossen, M., and H. Bujard. 1992. Tight control of gene expression in mammalian cells by tetracycline-responsive promoters. *Proc. Natl. Acad. Sci. USA.* 89: 5547–5551.

Gupta, A., L.H. Tsai, and A. Wynshaw-Boris. 2002. Life is a journey: a genetic look at neocortical development. *Nat. Rev. Genet.* 3:342–355.

Hafezparast, M., R. Klocke, C. Ruhrberg, A. Marquardt, A. Ahmad-Annuar, S. Bowen, G. Lalli, A.S. Witherden, H. Hummerich, S. Nicholson, et al. 2003. Mutations in dynein link motor neuron degeneration to defects in retrograde transport. *Science.* 300:808–812.

Harada, A., Y. Takei, Y. Kanai, Y. Tanaka, S. Nonaka, and N. Hirokawa. 1998. Golgi vesiculation and lysosome dispersion in cells lacking cytoplasmic dynein. *J. Cell Biol.* 141:51–59.

Hauri, H.P., F. Kappeler, H. Andersson, and C. Appenzeller. 2000. ERGIC-53 and traffic in the secretory pathway. *J. Cell Sci.* 113:587–596.

Hirotsune, S., M.W. Fleck, M.J. Gambelo, G.J. Bix, A. Chen, G.D. Clark, D.H. Ledbetter, C.J. McBain, and A. Wynshaw-Boris. 1998. Graded reduction of Pafah1b1 (lis1) activity results in neuronal migration defects and early embryonic lethality. *Nat. Genet.* 19:333–339.

Hirokawa, N. 1998. Kinesin and dynein superfamily proteins and the mechanism of organelle transport. *Science.* 279:519–526.

Holleran, E.A., S. Karki, and E.L.F. Holzbaur. 1998. The role of dynactin complex in intracellular motility. *Int. Rev. Cytol.* 182:69–109.

Howell, B.J., B.F. McEwen, J.C. Canman, D.B. Hoffman, E.M. Farrar, C.L. Rieder, and E.D. Salmon. 2001. Cytoplasmic dynein/dynactin drives kinetochore protein transport to the spindle poles and has a role in mitotic spindle checkpoint inactivation. *J. Cell Biol.* 155:1159–1172.

Jiang, W., and T. Hunter. 1998. Analysis of cell-cycle profiles in transfected cells using a membrane-targeted GFP. *Biotechniques.* 24:348–354.

Jordens, I., M. Fernandez-Borja, M. Marsman, S. Dusseljee, L. Janssen, J. Calafat, H. Janssen, R. Wubbolts, and J. Neefjes. 2001. The Rab7 effector protein RILP controls lysosomal transport by inducing the recruitment of dynein-dynactin motors. *Curr. Biol.* 11:1680–1685.

Karki, S., and E.L. Holzbaur. 1999. Cytoplasmic dynein and dynactin in cell division and intracellular transport. *Curr. Opin. Cell Biol.* 11:45–53.

Kauppi, M., A. Simonsen, B. Bremnes, A. Vieira, J. Callaghan, H. Stenmark, and V.M. Olkkonen. 2002. The small GTPase Rab22 interacts with EEA1 and controls endosomal membrane traffic. *J. Cell Sci.* 115:899–911.

Lippincott-Schwartz, J., C.Y. Lydia, S.B. Juan, and D.K. Richard. 1989. Rapid redistribution of Golgi proteins into the ER in cells treated with brefeldin A: evidence for membrane cycling from Golgi to ER. *Cell.* 56:801–813.

Lippincott-Schwartz, J., N.B. Cole, A. Marotta, P.A. Conrad, and G.S. Bloom. 1995. Kinesin is the motor for microtubule-mediated Golgi-to-ER membrane traffic. *J. Cell Biol.* 128:293–306.

Lodish, H., A. Berk, S.L. Zipursky, P. Matsudaira, D. Baltimore, and J.E. Darnell. 2000. Protein sorting: organelle biogenesis and protein secretion. *In* Molecular Cell Biology. S. Tenney, editor. W.H. Freeman and Company, New York. 675–750.

Lowe, M., C. Rabouille, N. Nakamura, R. Watson, M. Jackman, E. Jamsa, D. Rahman, D.J. Pappin, and G. Warren. 1998. Cdc2 kinase directly phosphorylates the cis-Golgi matrix protein GM130 and is required for Golgi fragmentation in mitosis. *Cell.* 94:783–793.

Mallet, W.G., and F.R. Maxfield. 1999. Chimeric forms of furin and TGN38 are transported with the plasma membrane in the trans-Golgi network via distinct endosomal pathways. *J. Cell Biol.* 146:345–359.

Matanis, T., A. Akhmanova, P. Wulf, E.D. Nery, T. Weide, T. Stepanova, N. Galjart, F. Grosveld, B. Goud, C.I. De Zeeuw, et al. 2002. Bicaudal-D regulates COPI-independent Golgi-ER transport by recruiting the dynein-dynactin motor complex. *Nat. Cell Biol.* 4:986–992.

Matteoni, R., and T.E. Kreis. 1987. Translocation and clustering of endosomes and lysosomes depends on microtubules. *J. Cell Biol.* 105:1253–1265.

Myers, J.W., J.T. Jones, T. Meyer, and J.E. Ferrell. 2003. Recombinant Dicer efficiently converts large dsRNAs into siRNAs suitable for gene silencing. *Nat. Biotechnol.* 21:324–328.

Niethammer, M., D.S. Smith, R. Ayala, J. Peng, J. Ko, M.S. Lee, M. Morabito, and L.H. Tsai. 2000. NUDEL is a novel Cdk5 substrate that associates with LIS1 and cytoplasmic dynein. *Neuron.* 28:697–711.

Presley, J.F., N.B. Cole, T.A. Schroer, K. Hirschberg, K.J. Zaal, and J. Lippincott-Schwartz. 1997. ER-to-Golgi transport visualized in living cells. *Nature.* 389:81–85.

Raub, T.J., M.J. Koroly, and R.M. Roberts. 1990. Endocytosis of wheat germ agglutinin binding sites from the cell surface into a tubular endosomal network. *J. Cell. Physiol.* 143:1–12.

Sasaki, S., A. Shionoya, M. Ishida, M.J. Gambello, J. Yingling, A. Wynshaw-Boris, and S. Hirotsune. 2000. A Lis1/NUDEL/cytoplasmic dynein heavy chain complex in the developing and adult nervous system. *Neuron.* 28:681–696.

Tai, C.Y., D.L. Dujardin, N.E. Faulkner, and R.B. Vallee. 2002. Role of dynein, dynactin, and CLIP-170 interactions in Lis1 kinetochore function. *J. Cell Biol.* 156:959–968.

Toyo-oka, K., A. Shionoya, M.J. Gambello, C. Cardoso, R. Leventer, H.L. Ward, R. Ayala, L.H. Tsai, W. Dobyns, D. Ledbetter, et al. 2003. 14-3-3epsilon is important for neuronal migration by binding to NUDEL: a molecular explanation for Miller-Dieker syndrome. *Nat. Genet.* 34:274–285.

Valetti, C., D.M. Wetzel, M. Schrader, M.J. Hasbani, S.R. Gill, T.E. Kreis, and T.A. Schroer. 1999. Role of dynactin in endocytic traffic: effects of dynamitin overexpression and colocalization with CLIP-170. *Mol. Biol. Cell.* 10: 4107–4120.

Virtanen, I., P. Ekblom, and P. Laurila. 1980. Subcellular compartmentalization of saccharide moieties in cultured normal and malignant cells. *J. Cell Biol.* 85:

429–434.

Wacker, I., C. Kaether, A. Kromer, A. Migala, W. Almers, and H.H. Gerdes. 1997. Microtubule-dependent transport of secretory vesicles visualized in real time with a GFP-tagged secretory protein. *J. Cell Sci.* 110:1453–1463.

Walker, W.H., S.L. Fitzpatrick, H.A. Barrera-Saldana, D. Resendez-Perez, and G.F. Saunders. 1991. The human placental lactogen genes: structure, function, evolution and transcriptional regulation. *Endocr. Rev.* 12:316–328.

Wang, P., Y.L. Wu, T.H. Zhou, Y. Sun, and G. Pei. 2000. Identification of alternative splicing variants of the beta subunit of human Ca(2+)/calmodulin-dependent protein kinase II with different activities. *FEBS Lett.* 475:107–110.

Willins, D.A., B. Liu, X. Xiang, and N.R. Morris. 1997. Mutations in the heavy chain of cytoplasmic dynein suppress the nudF nuclear migration mutation of *Aspergillus nidulans*. *Mol. Gen. Genet.* 255:194–200.

Wynshaw-Boris, A., and M.J. Gambello. 2001. Lis1 and dynein motor function in neuronal migration and development. *Genes Dev.* 15:639–651.

Xiang, X., S.M. Beckwith, and N.R. Morris. 1994. Cytoplasmic dynein is involved in nuclear migration in *Aspergillus nidulans. Proc. Natl. Acad. Sci. USA.* 91: 2100–2104.

Xiang, X., A.H. Osmani, S.A. Osmani, M. Xin, and N.R. Morris. 1995. NudF, a nuclear migration gene in *Aspergillus nidulans,* is similar to the human LIS-1 gene required for neuronal migration. *Mol. Biol. Cell.* 6:297–310.

Yan, X., F. Li, Y. Liang, Y. Shen, X. Zhao, Q. Huang, and X. Zhu. 2003. Human Nudel and NudE as regulators of cytoplasmic dynein in the poleward protein transport along the mitotic spindle. *Mol. Cell. Biol.* 23:1239–1250.

Yang, Z., J. Guo, N. Li, M. Qian, S. Wang, and X. Zhu. 2003. Mitosin/CENP-F is a conserved kinetochore protein subjected to cytoplasmic dynein-mediated poleward transport. *Cell Res.* 13:275–283.

Zhu, X. 1999. Structural requirements and dynamics of mitosin-kinetochore interaction in M phase. *Mol. Cell. Biol.* 19:1016–1024.